Perturbative series expansions: theoretical aspects and numerical investigations

Luca Biasco
Dipartimento di Matematica
Università di Roma Tre
Largo S. L. Murialdo 1, I-00146 Roma (Italy)
(biasco@mat.uniroma3.it)

Alessandra Celletti
Dipartimento di Matematica
Università di Roma Tor Vergata
Via della Ricerca Scientifica 1, I-00133 Roma (Italy)
(celletti@mat.uniroma2.it)

October 23, 2004

Abstract

Perturbation theory is introduced by means of models borrowed from Celestial Mechanics, namely the two–body and three–body problems. Such models allow to introduce in a simple way the concepts of integrable and nearly–integrable systems, which can be conveniently investigated using Hamiltonian formalism. After discussing the problem of the convergence of the Lindstedt series, we introduce the basic notions of KAM theory, which allows (under quite general assumptions) to state the persistence of invariant tori. The value at which such surfaces break–down can be determined by means of numerical algorithms. Among the others, we review three methods to which we refer as Greene, Padé and Lyapunov. We present some concrete applications to discrete models of the three different techniques, in order to provide complementary information about the break–down of invariant tori.

Keywords: Perturbation theory, KAM theorem, break–down threshold, invariant curves.

1 Introduction

The dynamics of the planets and satellites is ruled by Newton's law, according to which the gravitational force is proportional to the product of the masses of the interacting bodies and it is inversely proportional to the square of their distance. The description of the trajectories spanned by the celestial bodies starts with the simplest model in which one considers only the attraction exerted by the Sun, neglecting all contributions due to other planets or satellites. Such model is known as the *two–body problem* and it is fully described by Kepler's laws, according to which the motion is represented by a conic. Consider, for example, the trajectory of an asteroid moving on an elliptic orbit around the Sun. In the two–body aproximation the semimajor axis and the eccentricity of the ellipse are fixed in time. However, such example represents only the first approximation of the asteroid's motion, which is actually subject also

to the attraction of the other planets and satellites of the solar system. The most important contribution comes from the gravitational influence of Jupiter, which is the largest planet of the solar system, being its mass equal to 10^{-3} times the mass of the Sun. Therefore, next step is to consider the *three–body problem* formed by the Sun, the asteroid and Jupiter. A complete mathematical solution of such problem was hunted for since the last three centuries. A conclusive answer was given by H. Poincaré ([13]), who proved that the three–body problem does not admit a mathematical solution, in the sense that it is not possible to find explicit formulae which describe the motion of the asteroid under the simultaneous attraction of the Sun and Jupiter. For this reason, the three–body problem belongs to the class of non–integrable systems. However, since the mass of Jupiter is much smaller than the mass of the Sun, the trajectory of the asteroid will be in general weakly perturbed with respect to the Keplerian solution. In this sense, one can speak of the three–body problem as a nearly–integrable system (see section 3).
Let us consider a trajectory of the three–body problem with preassigned initial conditions. Though an explicit solution of such motion cannot be found, one can look for an approximate solution of the equations of motion by means of mathematical techniques ([2]) known as *perturbation theory* (see section 4), which can be conveniently introduced in terms of the Hamiltonian formalism reviewed in section 2. More precisely, one can construct a transformation of coordinates such that the system expressed in the new variables provides a better approximation of the true solution. The coordinate's transformations are builded up by constructing suitable series expansions, known as *Lindstedt series*, and a basic question (obviously) concerns their domain of convergence. In the context of perturbation theory, a definite breakthrough is provided by Kolmogorov's theorem, later extended by Arnold and Moser, henceforth known as KAM theory by the akronym of the authors ([10], [1], [12]). Let ε denote the perturbing parameter, such that for $\varepsilon = 0$ one recovers the integrable case (in the three–body problem the perturbing parameter is readily seen to represent the Jupiter–Sun mass–ratio). The novelty of KAM theory relies in fixing the frequency, rather than the initial conditions, and in using a quadratically convergent procedure of solution (rather than a linear one, like in classical perturbation theory). The basic assumption consists in assuming a strongly irrational (or diophantine) condition on the frequency ω. In conclusion, having fixed a diophantine frequency ω for the unperturbed system ($\varepsilon = 0$), KAM theory provides an explicit algorithm to prove the persistence, for a sufficiently small $\varepsilon \neq 0$, of an invariant torus on which a quasi–periodic motion with frequency ω takes place; moreover, Kolmogorov's theory proves that the set of such invariant tori has positive measure in the phase space.

KAM theorem provides a lower bound on the break–down threshold of the invariant torus with frequency ω, say $\varepsilon = \varepsilon_c(\omega)$. Nowadays there are several numerical techniques which allow to evaluate, with accurate precision, the transition value $\varepsilon_c(\omega)$. One of the most widely accepted methods was developed by Greene ([8]) and it is based on the conjecture that the break–down of the invariant torus with rotation number ω is related to the transition from stability to instability of the periodic orbits with frequency equal to the rational approximants to ω. We remark that such conjecture was partially justified in [7], [11].
Being the invariant torus described in terms of the Lindstedt series, it is definitely important to analyze the domain of convergence of such series in the complex parameter plane. Let us denote by $\rho_c(\omega)$ the radius of convergence of the Lindstedt series. Numerical experiments suggest that Greene's threshold coincides with the intersection of such domain with the positive real axis.

Whenever the domain of convergence deviates from a circle, the two thresholds $\varepsilon_c(\omega)$ and $\rho_c(\omega)$ may be markedly different. The domain of analyticity can be obtained by implementing Padé's method ([3]), which allows to approximate the Lindstedt series by the ratio of two polynomials. The zeros of the denominators provide the poles, which contribute to the determination of the analyticity domain. In order to evaluate the radius of convergence of the Lindstedt series one can apply an alternative technique developed in [5], to which we refer as Lyapunov's method, based on the computation of a quantity related to the numerical definition of Lyapunov's exponents, measuring the divergence of the Lindstedt series.

Concrete applications of Greene's, Padé's and Lyapunov's techniques are presented in sections 5 and 6 for a discrete model, known as the *standard map*. We consider also variants of such mapping (adding suitable Fourier components) and we analyze the behaviour of invariant curves with three different frequencies. Notice that the results (Tables and Figures) provided in sections 5 and 6 are taken from [5].

2 Hamiltonian formalism

Consider a smooth function $H := H(y,x)$ with $(y,x) \in M := \mathbf{R}^n \times \mathbf{R}^n$, $n = 1,2,3,\ldots$ and the following systems of O.D.E.'s:

$$\begin{aligned} \dot{y}(t) &= -H_x(y(t),x(t)) \ , \\ \dot{x}(t) &= H_y(y(t),x(t)) \end{aligned} \tag{2.1}$$

(here and in the following $H_x(y,x) \equiv \frac{\partial H}{\partial x}(x,y)$, $H_y(y,x) \equiv \frac{\partial H}{\partial y}(x,y)$). Define

$$\Phi_H^t(y_0,x_0) := (y(t),x(t))$$

as the solution at time t with initial data $y(0) := y_0$ and $x(0) := x_0$. We remark that the value of H along the solution of (2.1) is constant, i.e.

$$H(y(t),x(t)) \equiv H(y_0,x_0) =: E \tag{2.2}$$

for a suitable $E \in \mathbf{R}$. The function H is called *Hamiltonian*, M is the *phase space*, (2.1) are *Hamilton's equations* associated to H, Φ_H^t is the *Hamiltonian flow* of H at time t starting from (y_0,x_0) and (2.2) expresses the preservation of the energy.

An elementary example of the derivation of the Hamiltonian function associated to a mechanical model is provided by a pendulum. Consider a point of mass m, which keeps constant distance d from the origin of a reference frame. Suppose that the system is embedded in a weak gravity field of strength ε. Normalizing the units of measure so that $m = 1$ and $d = 1$, the Hamiltonian describing the motion is given by

$$H(r,\theta) = \frac{1}{2}r^2 + \varepsilon\cos\theta \ , \tag{2.3}$$

where $\theta \in \mathbf{T} \equiv \mathbf{R}/(2\pi\mathbf{Z})$ is the angle described by the particle with the vertical axis and $r \in \mathbf{R}$ is the velocity, i.e. $r = \dot{\theta}$. Being one–dimensional, the system can be easily integrated by quadratures.

Another classical example of a physical model which can be conveniently studied through Hamiltonian formalism, is provided by the harmonic oscillator. The equation governing the small oscillations (described by the coordinate $x \in \mathbf{R}$) of a body attached to the end of an elastic spring is given by Hooke's law, which can be expressed as

$$\ddot{x} = -\nu^2 x \ ,$$

for a suitable $\nu > 0$ representing the strength of the spring. The corresponding Hamiltonian is given by

$$H(y, x) = \frac{1}{2} y^2 + \frac{1}{2} \nu^2 x^2 \ ,$$

whose associated Hamilton's equations are

$$\dot{y} = -\nu^2 x \ , \qquad \dot{x} = y \ . \tag{2.4}$$

Equations (2.4) can be trivially solved as

$$\begin{aligned} y(t) &= -\alpha\nu \sin(\nu t + \beta) \ , \\ x(t) &= \alpha \cos(\nu t + \beta) \ , \end{aligned} \tag{2.5}$$

for suitable constants α, β related to the initial conditions $x(0)$, $y(0)$. It is rather instructive to use this example in order to introduce suitable coordinates, known as *action–angle variables,* which will play a key role in the context of perturbation theory. Indeed, we proceed to construct a change of coordinates $\Psi(I, \varphi) = (y, x)$, defined through the relation

$$\Phi^t_{H \circ \Psi} = \Phi^t_H \circ \Psi \ . \tag{2.6}$$

For $(y, x) \neq (0, 0)$, we can define the change of variables

$$\begin{aligned} y &= \sqrt{2\nu I} \cos \varphi \ , \\ x &= \sqrt{2I/\nu} \sin \varphi \ , \end{aligned} \tag{2.7}$$

where $I > 0$ and $\varphi \in \mathbf{T} := \mathbf{R}/(2\pi\mathbf{Z})$. Notice that the coordinate I has the dimension of an action[1], while φ is an angle. A trivial computation shows that the previous change of coordinates satisfies (2.6). Moreover, we remark that the new Hamiltonian

$$K := K(I) := H \circ \Psi(I, \varphi) = \nu \ I$$

does not depend on φ. Denoting by $\omega := \nabla K(I) \equiv \frac{\partial K(I)}{\partial I}$, equations (2.1) become

$$\dot{I} = 0 \ , \ \dot{\varphi} = \nu, \tag{2.8}$$

whose solution is given by

$$\begin{aligned} I(t) &\equiv I_0 \\ \varphi(t) &\equiv \nu t + \varphi_0 \ . \end{aligned} \tag{2.9}$$

[1] Namely energy×time.

Notice that inserting (2.9) in (2.7), one recovers the solution (2.5). In view of this example, we are led to the following

Definition: A change of coordinates Ψ verifying (2.6) is said to be *canonical*. The coordinates $(I, \varphi) \in M$ (where the phase space is $M := \mathbf{R}^n \times \mathbf{T}^n$ with $\mathbf{T}^n := \mathbf{R}^n/(2\pi\mathbf{Z})^n$) are called *action–angle variables*.

Notice that if the Hamiltonian H is expressed in terms of action–angle variables, namely $H = H(I, \varphi)$, then equations (2.1) become

$$\dot{I}(t) = -H_\varphi(I(t), \varphi(t)) \ , \qquad \dot{\varphi}(t) = H_I(I(t), \varphi(t)) \ . \tag{2.10}$$

3 Integrable and nearly–integrable systems

Let us consider a Hamiltonian function expressed in action–angle variables, namely $H = H(I, \varphi)$, where $(I, \varphi) \in M := \mathbf{R}^n \times \mathbf{T}^n$. A system described by a Hamiltonian H, which does not depend on the angles, namely

$$H(I, \varphi) = h(I)$$

for a suitable function h, is said to be (completely) integrable. For these systems, Hamilton's equations can be written as $\dot{I} = 0$, $\dot{\varphi} = \nabla h(I)$. Correspondingly, we introduce the *invariant*[2] *tori*

$$\mathbf{T}_{\omega_0} := \{(I, \varphi) \mid I \equiv I_0 \ , \quad \varphi \in \mathbf{T}^n\} \ ,$$

run by the linear flow $\varphi(t) = \omega_0 t + \varphi_0$, with $\omega_0 := \nabla h(I_0) \in \mathbf{R}^n$. If the frequency ω_0 is rationally independent (i.e., $\omega_0 \cdot k \neq 0$ for all $k \in \mathbf{Z}^n \setminus \{0\}$), the torus $\mathbf{T}_{\omega_0}$ is called non–resonant and it is densely filled by the flow $t \to \omega_0 t + \varphi_0$. In this case, the flow is said to be quasi–periodic. If the frequency ω_0 is rationally dependent, the torus is called resonant (and it is foliated by lower dimensional invariant tori). We remark that this case is highly degenerate, since the probability to have a rationally dependent frequency is zero.

In the previous statements we have fully classified all motions associated to integrable Hamiltonian systems. A more difficult task concerns the study of systems which are close to integrable ones. More precisely, consider a weak perturbation of an integrable Hamiltonian $h(I)$: denoting by $\varepsilon \in \mathbf{R}$ the size of the perturbation, we can write a perturbed system as

$$H(I, \varphi; \varepsilon) := h(I) + \varepsilon f(I, \varphi; \varepsilon) \ , \tag{3.11}$$

where $(I, \varphi) \in M := \mathbf{R}^n \times \mathbf{T}^n$, f is a smooth function and the real parameter ε is small, i.e. $0 < \varepsilon < 1$. The equations of motion (2.10) become

$$\begin{aligned} \dot{I}(t) &= -\varepsilon \frac{\partial f}{\partial \varphi}(I(t), \varphi(t); \varepsilon) \ , \\ \dot{\varphi}(t) &= \nabla h(I(t)) + \varepsilon \frac{\partial f}{\partial I}(I(t), \varphi(t); \varepsilon) \ . \end{aligned} \tag{3.12}$$

[2] Namely $\Phi_H^t(\mathbf{T}_{\omega_0}) \subseteq \mathbf{T}_{\omega_0}$.

Mechanical systems described by Hamiltonian functions of the form (3.11) are called *nearly–integrable*, since for $\varepsilon = 0$ equations (3.12) can be trivially integrated (compare with (2.8), (2.9)).

In order to provide explicit examples of integrable and nearly–integrable Hamiltonian systems, we recall in the following subsections the celebrated two–body and three–body problems.

3.1 The two–body problem

Consider the motion of an asteroid A orbiting around the Sun S, which is assumed to coincide with the origin of a fixed reference frame. Suppose to neglect the gravitational interaction of the asteroid with the other objects of the solar system. The two–body asteroid–Sun motion is described by Kepler's laws, which ensure that for negative energy the orbit of the asteroid around the Sun is an ellipse with the Sun located at one of the two foci. The Hamiltonian formulation of the two–body problem is described as follows. Choose the units of length, mass and time so that the gravitational constant and the mass of the Sun are normalized to one. In order to investigate the asteroid–Sun problem, it is convenient to introduce suitable coordinates, known as Delaunay variables:

$$(I_1, I_2) \equiv (L, G) \in \mathbf{R}^2 \ , \qquad (\varphi_1, \varphi_2) \equiv (l, g) \in \mathbf{T}^2 \ ,$$

whose definition is the following. Denoting by a and e, respectively, the semimajor axis and eccentricity of the orbit of the asteroid, the Delaunay actions are:

$$L := \sqrt{a} \ , \qquad G := \sqrt{a(1-e^2)} \ . \tag{3.13}$$

The conjugated angle variables are defined as follows: l is the *mean anomaly,* which provides the position of the asteroid along its orbit and g is the *longitude of perihelion,* namely the angle between the perihelion line and a fixed reference direction (see [14]).
The Hamiltonian function in Delaunay variables can be written as

$$H(L, G, l, g) := h(L) := -\frac{1}{2L^2} \ , \tag{3.14}$$

which shows that the system is integrable, since $H = h(L)$ depends only on the actions. From the equations of motion $\dot{L} = 0$, $\dot{G} = 0$, we immediately recognize that L and G are constants, $L = L_0$, $G = G_0$, which in view of (3.13) is equivalent to say that the orbital elements (semimajor axis and eccentricity) do not vary along the motion. Being also g constant ($\dot{g} = 0$), we obtain that the orbit is a fixed ellipse with one of the foci coinciding with the Sun. Finally, the mean anomaly is obtained from $\dot{l} = \frac{\partial H(L)}{\partial L} := \omega(L)$ as $l(t) = \omega(L_0)t + l(0)$.
Let us remark that the Hamiltonian (3.14) does not depend on all the actions, being independent on G: such kind of systems are called *degenerate* and often arise in Celestial Mechanics.

3.2 The three–body problem

The two–body problem describes only a rough approximation of the motion of the asteroid around the Sun; indeed, the most important contribution we neglected while considering Kepler's model comes from the gravitational influence of Jupiter. We are thus led to consider the motion of the three bodies: the Sun (S), Jupiter (J) and a minor body of the asteroidal belt

(A). We restrict our attention to the special case of the *planar, circular, restricted three–body problem.* More precisely, we assume that the Sun and Jupiter revolve around their common center of mass, describing circular orbits (circular case). Choose the units of length, mass and time so that that the gravitational constant, the orbital angular velocity and the sum of the masses of the primaries (Sun and Jupiter) are identically equal to one. Consider the motion of an asteroid A moving in the same orbital plane of the primaries (planar case). Assume that the mass of A is negligible with respect to the masses of S and J; this hypotheses implies that the motion of the primaries is not affected by the gravitational attraction of the asteroid (restricted case). Finally, let us identify the mass of J with a suitable small parameter ε. Though being the simplest (non trivial) three–body model, as shown by Poincaré ([13]) such problem cannot be explicitly integrated (like the two–body problem through Kepler's solution). In order to introduce the Hamiltonian function associated to such problem, it is convenient to write the equations of motion in a barycentric coordinate frame (with origin at the center of mass of the Sun–Jupiter system), which rotates uniformly at the same angular velocity of the primaries. The resulting system is described by a nearly–integrable Hamiltonian function with two degrees of freedom (see [14]) with the perturbing parameter ε representing the Jupiter–Sun mass–ratio.

We immediately recognize that for $\varepsilon = 0$ (i.e., neglecting Jupiter), the system reduces to the unperturbed two–body problem. As described in the previous section, we can identify the Delaunay elements with action–angle variables; the only difference is that in the rotating reference frame the variable g represents the longitude of the pericenter, evaluated from the axis coinciding with the direction of the primaries. If $H = h^{(AS)}(L)$ denotes the Hamiltonian function associated to the asteroid–Sun problem, it can be shown ([14]) that the Hamiltonian describing the three–body problem has the form

$$H(L, G, l, g; \varepsilon) := h^{(AS)}(L) - G + \varepsilon f(L, G, l, g; \varepsilon) \ , \tag{3.15}$$

for a suitable analytic function f, which represents the interaction between the asteroid and Jupiter. The Hamiltonian (3.15) is a prototype of a nearly–integrable system, since the integrable two–body problem is recovered as soon as the perturbing parameter ε is set equal to zero.

The action–angle formalism provides a standard tool to solve explicitly the equations of motion associated to integrable systems; on the other side, one could expect that for small perturbations the behaviour of nearly–integrable systems is similar to the integrable ones. By (3.12) this remark is obviously true as long as the time is less than $1/\varepsilon$, though the question remains open for longer time scales. In order to face this problem, one could naively try to perform a change of variables, which transforms the nearly–integrable system (3.11) into a trivially integrable one (at least for ε small enough). However, a natural question concerns the existence of a canonical transformation $\Psi := (J, \psi) \to (I, \varphi)$ such that on a given time scale the nearly–integrable Hamiltonian system (3.11) is transformed into a new Hamiltonian system, $K := H \circ \Psi$, which does not depend on the new angle coordinates on a given time scale; perturbation theory will provide a tool to investigate such strategy of approaching nearly–integrable systems.

4 Perturbation theory

Perturbation theory flowered during the last two centuries through the works of Laplace, Leverrier, Delaunay, Poincaré, Tisserand, etc.; it provides constructive methods to investigate the behaviour of nearly–integrable systems. The importance of studying the effects of small Hamiltonian perturbations on an integrable system was pointed out by Poincaré, who referred to it as the *fundamental problem of dynamics*. We introduce perturbation theory in section 4.1 by means of the *Lindstedt method* and we present in section 4.2 the celebrated Kolmogorov–Arnold–Moser theorem.

4.1 Lindstedt method

Consider an analytic Hamiltonian of the form

$$H(I,\varphi;\varepsilon) := h(I) + \varepsilon f(I,\varphi;\varepsilon) \ , \tag{4.16}$$

where $I \in B_R := \{I \in \mathbf{R}^n \ , \ \ |I| \leq R\}$, $\varphi \in \mathbf{T}^n$ and $|\varepsilon| \leq \bar{\varepsilon}$ for suitable real constants $R > 0$, $\bar{\varepsilon} > 0$. Let us expand f in Taylor series of ε as

$$f(I,\varphi;\varepsilon) =: \sum_{j\geq 0} \varepsilon^j f^{(j)}(I,\varphi) \ ,$$

for suitable functions $f^{(j)}(I,\varphi)$, which can be expanded in Fourier series as $f^{(j)}(I,\varphi) = \sum_{k\in\mathbf{Z}^n} f_k^{(j)}(I) e^{ik\cdot\varphi}$. We implement an integrating transformation

$$\Psi : (J,\psi) \longmapsto (I,\varphi) \ ,$$

defined by the implicit equations

$$I = J + \varepsilon \partial_\varphi S(J,\varphi;\varepsilon) \ , \qquad \psi = \varphi + \varepsilon \partial_J S(J,\varphi;\varepsilon) \ , \tag{4.17}$$

where we have introduced the so–called Lindstedt series as

$$S(J,\varphi;\varepsilon) = \sum_{j\geq 0} \varepsilon^j S^{(j)}(J,\varphi;\varepsilon)$$

for suitable analytic functions $S^{(j)}$ to be determined as follows.
By the implicit function theorem it is simple to prove that, for ε small enough, (4.17) defines a good diffeomorphism, which is also canonical. We want to determine recursively $S^{(j)}$ so that the function $K := H \circ \Psi$ does not depend on ψ:

$$\Psi(J,\psi) = (J + \varepsilon \frac{\partial S^{(0)}(J,\psi;\varepsilon)}{\partial \varphi} + O(\varepsilon^2), \ \psi + O(\varepsilon)) \ .$$

To this end, we start by expanding $H \circ \Psi$ as

$$(H\circ\Psi)(J,\psi) = h(J) + \varepsilon \Big[\nabla h(J) \cdot \partial_\varphi S^{(0)}(J,\psi;\varepsilon) + f^{(0)}(J,\psi)\Big] + O(\varepsilon^2) \ . \tag{4.18}$$

We look for $S^{(0)}$ so that the term of order ε does not depend on the angles; we are thus led to the equation

$$\nabla h(J) \cdot \partial_\varphi S^{(0)}(J,\psi;\varepsilon) + f^{(0)}(J,\psi) = h^{(1)}(J;\varepsilon) \ , \tag{4.19}$$

where $h^{(1)}(J;\varepsilon) \equiv f_0^{(0)}(J)$ and

$$S^{(0)}(J,\varphi) := i \sum_{k\neq 0} \frac{f_k^{(0)}(J)}{\nabla h(J)\cdot k} e^{ik\cdot\varphi} \ . \tag{4.20}$$

The above expression contains a quantity at the denominator to which we refer as the *small divisor*, since it can become arbitrarily small:

$$\nabla h(J) \cdot k \ . \tag{4.21}$$

Indeed, the function $S^{(0)}$ can be defined only for values of the actions such that the small divisors (4.21) are different from zero, namely only for J belonging to the set of rational independent frequencies

$$\aleph := \{J \in \mathbf{R}^n \ , \quad \text{such that} \quad \nabla h(J) \cdot k \neq 0 \ , \ \forall\, k \in \mathbf{Z}^n \setminus \{0\}\} \ .$$

Since $\aleph$ has empty interior, if we want to define $S^{(0)}$ in an open neighborhood of a fixed $J_0 \in \aleph$, we must truncate the series in (4.20) up to a suitable order, say $|k| \leq d_0$ for a given $d_0 \in \mathbf{Z}_+$. In particular, let us write the Fourier expansion of $f^{(0)}$ as

$$f^{(0)}(J, \psi) = \sum_{|k| \leq d_0} f_k^{(0)}(J) e^{ik \cdot \psi} + \sum_{|k| > d_0} f_k^{(0)}(J) e^{ik \cdot \psi} \ ; \tag{4.22}$$

choosing a sufficiently large value of the truncation index $d_0 := d_0(\varepsilon)$, we can make the second sum in (4.22) of order ε, so that it will finally contribute to the $O(\varepsilon^2)$–term in the development (4.18). In summary, we have eliminated the angles in the expression (4.18) up to $O(\varepsilon)$ by using the transformation associated to $S^{(0)}$, which is defined for $J \in B_{\rho_0}(J_0)$, for a sufficiently small $\rho_0 := \rho_0(\varepsilon)$ such that no zero–divisors will occur, i.e.

$$\nabla h(J) \cdot k \neq 0 \ , \quad \forall\, 0 < |k| \leq d_0(\varepsilon) \ , \quad J \in B_{\rho_0(\varepsilon)}(J_0) \ .$$

In order to eliminate the angle dependence in (4.18) for the terms of order $\varepsilon^2, \varepsilon^3, \ldots, \varepsilon^{m+1}, \ldots$, we determine $S^{(1)}$, $S^{(2)}$, …, $S^{(m)}$, …, by solving equations similar to (4.19). Again, we need to truncate the series associated to $S^{(m)}$ at the orders $|k| \leq d_m$ for sufficiently large indexes

$$d_m := d_m(\varepsilon) \ \longrightarrow \infty \quad \text{for} \quad m \to \infty \ .$$

Therefore, $S^{(m)}$ will be defined only for $J \in B_{\rho_m}(J_0)$ for sufficiently small values of the radii, such that

$$\rho_m := \rho_m(\varepsilon) \ \longrightarrow 0 \quad \text{for} \quad m \to \infty \ .$$

As a consequence, the domains of definition of the functions $S^{(0)}$, $S^{(1)}$, …, $S^{(m)}$, … will drastically shrink to 0 as m increases.

Finally, iterating infinitely many times the above procedure we can formally write the resulting Hamiltonian function as

$$K(J; \varepsilon) := H \circ \Psi(J, \psi; \varepsilon) = h(J) + \varepsilon h_\infty(J; \varepsilon) \ ,$$

for a suitable function h_∞. However, we are immediately faced with the problem of the convergence of such procedure, namely with the question of the existence of $J_0 \in \aleph$ and $\varepsilon_0 > 0$, such that $K(J_0; \varepsilon)$ is well–defined for $|\varepsilon| \leq \varepsilon_0$. In general, as shown by Poincaré, the answer to this question is negative, as the following example of a diverging Lindstedt series shows.

Consider the Hamiltonian

$$H(I, \varphi; \varepsilon) := \omega \cdot I + \varepsilon \left[I_1 + \sum_{k \in \mathbf{N} \setminus \{\mathbf{0}\}} a_k \sin(k \cdot \varphi) \right] \ , \tag{4.23}$$

$(I,\varphi) \in \mathbf{R}^2 \times \mathbf{T}^2$, where $a_k := \exp(-|k|)$ and $\omega = (\omega_1, \omega_2)$, $\omega_1 < 0$, $\omega_2 > 0$ with $\omega_1/\omega_2 \in \mathbf{R} \setminus \mathbf{Q}$. For $\varepsilon = 0$ the phase space is foliated by non–resonant invariant tori, wrapped by the quasi–periodic flow $t \to \omega t + \varphi_0$. In this example, it is very simple to evaluate the Lindstedt series at any order, though it is not necessary for our purposes. Indeed, we just notice that if the Lindstedt series converges, we can define the canonical transformation $\Psi_\varepsilon : (J,\psi) \to (I,\varphi)$, which integrates the system, i.e. $H \circ \Psi_\varepsilon(J,\psi) =: K(J;\varepsilon)$. Therefore, from (2.6) the values of I_1 and I_2 remain bounded in time, since J is a constant vector. On the other hand, we can readily integrate (4.23) and in particular we have $\varphi_1(t) = (\omega_1 + \varepsilon)t + \varphi_1(0)$ and $\varphi_2(t) = \omega_2 t + \varphi_2(0)$, so that the solution for I_1 (with initial condition $\varphi(0) = 0$) is given by

$$I_1(t) = I_1(0) - \varepsilon \sum_{k \in \mathbf{N}/\{0\}} a_k \; k_1 \int_0^t \cos\Big(((\omega_1 + \varepsilon)k_1 + \omega_2 k_2)t\Big)\, dt \;, \tag{4.24}$$

which can be solved by quadratures. Moreover, whenever

$$\frac{\omega_1 + \varepsilon}{\omega_2} = \frac{p}{q} \qquad \text{for some} \quad p \in \mathbf{Z} \;,\; q \in \mathbf{N} \;,$$

the sum in (4.24) over all the terms with $(k_1, k_2) \neq (-q, p)$ gives a uniformly bounded contribution (for any $t \in \mathbf{R}$), while the term with $(k_1, k_2) = (-q, p)$ gives a contribution which goes to $\pm\infty$ when $t \to \pm\infty$, since we identically have

$$(\omega_1 + \varepsilon)k_1 + \omega_2 k_2 = 0 \;.$$

This computation allows to conclude that the Lindstedt series diverges.

As a final remark, we note that if the Lindstedt series converges for some $J_0 \in \aleph$ and $|\varepsilon| \leq \varepsilon_0$, then for any $|\varepsilon| \leq \varepsilon_0$ the perturbed system admits the invariant torus

$$\mathcal{T}_{\omega_0} := \Big\{ \Psi(J_0, \psi; \varepsilon) \;,\;\; \psi \in \mathbf{T}^n \Big\}$$

with frequency $\omega_0 := \nabla K(J_0; \varepsilon)$. In general, the rational dependence of the vector ω_0 will vary according to the values of ε. Therefore the torus $\mathcal{T}_{\omega_0}$ will be non–resonant or resonant according to the values of ε. As we have seen before, a resonant torus is foliated into lower dimensional tori; actually, this situation is highly degenerate and it determines the intrinsic reason for the divergence of the Lindstedt series.

4.2 KAM theory

The Kolmogorov–Arnold–Moser (KAM) theory provides a constructive method to investigate nearly–integrable Hamiltonian systems ([10], [1], [12]). In analogy to Lindstedt method, the basic idea relies on the elimination of the angle variables through suitable changes of coordinates, with the further requirement that the sequence of transformations will be *quadratically* convergent. Ignoring the size of the contribution of the small divisors, after performing the m–th change of coordinates the part of the remainder which depends on the angle variables will be of order ε^{2^m}. The crucial point in KAM theory is that this superconvergent estimate of the remainder terms counteracts the influence of the small divisors in a suitable nonresonant set. Indeed, the second ingredient of KAM theory is to focus on a given strongly rationally independent frequency, rather than on a given action.

To be more precise, consider an analytic Hamiltonian of the form (4.16). Fix a rationally independent frequency vector ω_0, such that $\omega_0 := \nabla h(J_0)$ for a suitable $J_0 \in \mathbf{R}^n$. We perform a canonical change of variables Ψ_1, implicitly defined as in (4.17) with $S = S^{(0)}$, where $S^{(0)}$ can be determined as in the Lindstedt method. Due to the strongly rational independence of ω_0, for $J \approx J_0$ the following estimate on the small divisors holds

$$|\nabla h(J) \cdot k| \approx |\omega_0 \cdot k| \gg 0 \ . \tag{4.25}$$

The transformed Hamiltonian becomes

$$\mathcal{K}_1 := H \circ \Psi_1 = h(J) + \varepsilon h^{(1)}(J; \varepsilon) + \varepsilon^2 \mathcal{R}_2(J, \psi; \varepsilon)$$

for a suitable remainder function $\mathcal{R}_2$.
Next step is substantially different from the corresponding case in Lindstedt method; let $h^*(J;\varepsilon) := h(J)+ \varepsilon h^{(1)}(J;\varepsilon)$ be the integrable part and let $\varepsilon^2 \mathcal{R}_2(J, \psi; \varepsilon)$ be the perturbation. The crucial advantage is that after one transformation the new perturbative parameter is $\delta := \varepsilon^2$ with Hamiltonian $\mathcal{K}_2 = h^* + \delta \mathcal{R}_2$. Then we introduce a second canonical change of variables Ψ_2, defined in a neighborhood of a suitable $J_1(\varepsilon)$ which is chosen to satisfy $\nabla h^*(J_1(\varepsilon); \varepsilon) = \omega_0$; this relation will ensure a good estimate on the small divisors as in (4.25). For ε small enough, we can find $J_1(\varepsilon)$ by the implicit function theorem, if we assume that

$$\det h''(J_0) \neq 0 \ . \tag{4.26}$$

It is easy to see that after the last change of variables the new remainder term will be of order $\delta^2 = \varepsilon^{2^2}$.

Iterating this procedure, at the m–step the angle–depending remainder will be of order ε^{2^m}. Finally, applying infinitely many times the KAM scheme, we end up with an integrable Hamiltonian of the form

$$\mathcal{K}(\mathcal{J}; \varepsilon) := H \circ \Psi_1 \circ \Psi_2 \circ \ldots =: H \circ \Psi_\infty(\mathcal{J}, \phi; \varepsilon) \ ,$$

which is defined for $\mathcal{J} = J_\infty(\varepsilon)$ and it satisfies

$$\nabla \mathcal{K}(J_\infty(\varepsilon); \varepsilon) = \omega_0 \ .$$

We have thus proved the existence of the invariant torus

$$\mathcal{T}_{\omega_0} := \Big\{ \Psi_\infty(J_\infty(\varepsilon), \phi; \varepsilon) \ , \quad \phi \in \mathbf{T}^n \Big\} \ ,$$

provided that the overall procedure converges on a non trivial domain.

Remark 4.1 Before stating the KAM theorem, let us summarize the main differences between the Lindstedt and KAM procedures.
Concerning Lindstedt method we recall that:

(1) after the m–th coordinate's transformation the remainder term (depending upon angles) is of order ε^{m+1},

(2) the initial datum J_0 is kept fixed, while the final frequency $\nabla h(J_0;\varepsilon)$ (respectively the invariant surface $\mathbf{T}_{\nabla h(J_0;\varepsilon)}$) varies with ε, eventually becoming rationally dependent (respectively, a resonant torus).

Concerning the KAM procedure we recall that:

(1) after the m–th coordinate's transformation the remainder term (depending upon angles) is of order ε^{2^m},

(2) the frequency vector ω_0 is fixed and it is supposed to be strongly rational independent, so that the corresponding torus $\mathbf{T}_{\omega_0}$ is strongly non resonant.

We now proceed to state the KAM theorem as follows. Consider a Hamiltonian system as in (3.11). As we discussed previously, for $\varepsilon = 0$ the phase space of the unperturbed (integrable) system h is foliated by n–dimensional invariant tori labelled by $I = I_0$. Such tori are resonant or nonresonant according to the fact that the frequency $\omega_0 := \nabla h(I_0)$ is rationally dependent or not. KAM theorem describes the fate of nonresonant tori under perturbation. We recall that the three assumptions necessary to prove the theorem are the following: the smallness of ε, the strongly rational independence of ω_0 and the nondegeneracy of the unperturbed Hamiltonian h as given in (4.26).

KAM Theorem. *If the unperturbed system is nondegenerate, then, for a sufficiently small perturbation, most nonresonant invariant tori do not break–down, though being deformed and displaced with respect to the integrable situation. Therefore, in the phase space of the perturbed system there exist invariant tori densely filled with quasi–periodic phase trajectories winding around them. These invariant tori form a majority, in the sense that the measure of the complement of their union is small when the perturbation is small.*

The proof of the KAM theorem is based on the superconvergent procedure described above. We remark that the strongly rational independence of ω_0 (see (4.25)) plays a central role. In particular, the KAM scheme works if ω_0 satisfies the so–called Γ–τ *Diophantine condition*

$$|\omega_0 \cdot k| \geq \frac{\Gamma}{|k|^\tau} \ , \quad \forall\ k \in \mathbf{Z}^n \setminus \{0\} \ , \tag{4.27}$$

for a suitable $\Gamma = \Gamma(\varepsilon) > 0$ and $\tau > n - 1$.
More precisely, it results that all tori having Γ–τ Diophantine frequency vector with

$$\Gamma > const. \times \sqrt{\varepsilon}$$

are preserved under the perturbation.
We remark that the KAM result is global, in the sense that for all $\varepsilon \leq \varepsilon_0$ (ε_0 fixed) and for all Γ–τ Diophantine frequency vectors ω_0 satisfying (4.27), the Hamiltonian system (3.11) admits an invariant perturbed torus with frequency vector ω_0.

It is worth stressing that KAM theorem can be also stated as follows. Consider an unperturbed ($\varepsilon = 0$) surface with a fixed diophantine frequency ω_0 and look at its fate when the perturbation is switched on ($\varepsilon > 0$). Then, for ε small enough, the torus persists, being deformed and displaced with respect to the integrable limit, until the perturbing parameter ε reaches a threshold $\varepsilon_c := \varepsilon_c(\omega_0)$ at which the surface is destroyed (i.e., it looses regularity). For low–dimensional systems, KAM theory allows to prove a strong stability result concerning the confinement of the action variables in phase space.

Theorem. *In a non–degenerate system with two degrees of freedom, for $\varepsilon \leq \varepsilon_0$ (for a suitable sufficiently small $\varepsilon_0 > 0$) and for all initial conditions, the values of the actions remain forever near their initial values.*

The above statement is based on the following remark. For a two degrees of freedom Hamiltonian system, the phase space is four–dimensional, the energy level sets (on which the motion takes place) are three–dimensional, while the KAM tori are two–dimensional, filling a large part of each energy level. Any orbit starting in the region between two invariant tori remains forever trapped in it.

As an immediate corollary of the previous theorem, the stability of the actions in the planar, circular, restricted three–body problem follows. Using the original versions of Arnold's theorem, M. Hénon ([9]) proved the existence of invariant tori provided that the perturbing parameter is less than 10^{-333}; this value can be improved by implementing Moser's theorem, which yields an estimate of the order of 10^{-50}. We recall that the perturbing parameter represents the ratio of the masses of Jupiter and the Sun; its astronomical value amounts to about 10^{-3}.
Accurate analytical estimates based on a computer–assisted implementation allow to drastically improve such results by showing the existence of invariant tori on a preassigned energy level for parameter values less or equal than 10^{-3}, in agreement with the physical measurements (see [4] for further details).

5 A discrete model: the standard map

In the previous sections we focussed our attention on *continuous* systems; now we want to introduce *discrete* systems, which can be viewed as surfaces of section of Hamiltonian flows. Such models are definitely simpler than continuous systems, since their evolution can be known without introducing any numerical error due to integration algorithms. Let us start by considering the familiar pendulum model described by equation (2.3). In order to compute numerically the trajectory associated to Hamilton's equations for (2.3), i.e.

$$\begin{aligned} \dot{r} &= \varepsilon \sin\theta \\ \dot{\theta} &= r \ , \end{aligned} \tag{5.28}$$

we can use a leap–frog method, such that if T is the time–step and (r_n, θ_n) denotes the solution at time nT, then (5.28) can be integrated as

$$\begin{aligned} r_{n+1} &= r_n + T\varepsilon \sin\theta_n \\ \theta_{n+1} &= \theta_n + T r_{n+1} \ . \end{aligned}$$

Normalizing the time–step to one, we are reduced to the study of the so–called *standard map* introduced by Chirikov in ([6]):

$$\begin{aligned} r_{n+1} &= r_n + \varepsilon \sin\theta_n \\ \theta_{n+1} &= \theta_n + r_{n+1} \ , \end{aligned} \tag{5.29}$$

with $r_n \in \mathbf{R}$ and $\theta_n \in \mathbf{T} \equiv \mathbf{R}/(2\pi\mathbf{Z})$. We will also consider the generalized standard map, which is obtained replacing the sine term in (5.29) by any periodic, continuous function $f(\theta)$:

$$\begin{aligned} r_{n+1} &= r_n + \varepsilon f(\theta_n) \\ \theta_{n+1} &= \theta_n + r_{n+1} = \theta_n + r_n + \varepsilon f(\theta_n) \ , \end{aligned} \tag{5.30}$$

where $r_n \in \mathbf{R}$ and $\theta_n \in \mathbf{T} \equiv \mathbf{R}/(2\pi\mathbf{Z})$. We notice that the Jacobian associated to (5.30) is identically one, being the map area–preserving. We remark also that for $\varepsilon = 0$ the mapping reduces to a simple rotation, i.e.

$$\begin{aligned} r_{n+1} &= r_n = r_0 \\ \theta_{n+1} &= \theta_n + r_0 \ . \end{aligned}$$

We refer to $\omega \equiv r_0$ as the *frequency* or *rotation number* of the unperturbed mapping, which is generally defined as

$$\omega \equiv \lim_{n\to\infty} \frac{\theta_n}{n} \ .$$

If $\omega \in \mathbf{Q}$, the trajectory described by the iteration of the mapping with initial data (r_0, θ_0) is a periodic orbit; if $\omega \in \mathbf{R}\backslash\mathbf{Q}$, the motion takes place on an invariant curve with frequency ω, say $\mathcal{C}_{0,\omega}$. When $\varepsilon \neq 0$ the system becomes non–integrable and we proceed to describe the conclusions which can be drawn by applying perturbation theory. As we described in the previous sections, KAM theorem ([10], [1], [12]) ensures that if ε is sufficiently small, there still exists for the perturbed system an invariant curve $\mathcal{C}_{\varepsilon,\omega}$ with frequency ω. The KAM theorem can be applied provided that the frequency ω satisfies a strong irrationality assumption, namely the diophantine condition (4.27), which can now be rephrased as

$$|\frac{\omega}{2\pi} - \frac{p}{q}| \ \geq \ \frac{1}{Cq^2} \ , \qquad \forall p, q \in \mathbf{Z}/\{0\},$$

for some positive constant C. As the perturbing parameter is increased, the invariant curve becomes more and more distorted and displaced, until one reaches a critical value at which $\mathcal{C}_{\varepsilon,\omega}$ breaks–down. Let us define the critical break–down threshold $\varepsilon_c(\omega)$ as the supremum of the positive values of ε, such that there still exists an invariant curve with rotation number ω.

We provide a mathematical definition of $\mathcal{C}_{\varepsilon,\omega}$ as the invariant curve described by the parametric equations

$$\begin{aligned} r_n &= \omega + U(\varphi_n) - U(\varphi_n - \omega) \ , \\ \theta_n &= \varphi_n + U(\varphi_n) \ , \end{aligned} \tag{5.31}$$

where $\varphi_n \in \mathbf{T}$ and the conjugating function $U(\varphi_n)$ is 2π–periodic and analytic in ε; moreover, the parametrization is defined so that the flow is linear, i.e. $\varphi_{n+1} = \varphi_n + \omega$.
The function U can be expanded as a Taylor series in ε and a Fourier series in φ (the so–called Lindstedt series) as

$$U(\varphi_n) \ \equiv \ \sum_{j=1}^{\infty} \varepsilon^j U_j(\varphi_n) \ = \ \sum_{j=1}^{\infty} \varepsilon^j \sum_{l\in\mathbf{Z}} \hat{U}_{lj} e^{il\varphi_n}$$

for suitable Taylor coefficients U_j and Fourier–Taylor coefficients $\hat{U}_{lj}$. We define the *radius of convergence* of the Lindstedt series as

$$\rho_c(\omega) \;=\; \inf_{\varphi\in\mathbf{T}} (\limsup_{j\to\infty} |U_j(\varphi)|^{1/j})^{-1} \;.$$

We intend to study the relation between the two quantities $\varepsilon_c(\omega)$ and $\rho_c(\omega)$ in the complex parameter space (i.e., taking $\varepsilon \in \mathbf{C}$). In particular, we want to investigate the shape of the domain of convergence of the Lindstedt series and the location of the complex singularities. This task will be performed by looking at the behaviour of the periodic orbits, which approach more closely the invariant curve with frequency ω. We stress that if the domain of analyticity is not a circle, then the analyticity radius and the critical break–down threshold might be very different.

The tools adopted to investigate the shape of the analyticity domains are based on different methods: Greene's technique ([8]), the computation of Padé approximants and a recent method developed in [5].

5.1 Link between periodic orbits and invariant curves

In order to familiarize with the concepts of periodic orbits and invariant curves, let us consider a specific example provided by the mapping (5.29) and by the invariant curve with frequency proportional to the golden ratio: $\omega = 2\pi\,\frac{\sqrt{5}-1}{2}$. As it is well known, the golden ratio is approximated by the sequence of Fibonacci's numbers $\{\frac{F_k}{F_{k+1}}\} \in \mathbf{Q}$, defined as

$$F_{k+1} = F_k + F_{k-1} \quad (k \geq 1) \qquad \text{with} \qquad F_0 = 0, \quad F_1 = 1 \;.$$

Figure 1 shows in the (θ, r)–plane (with θ normalized by a factor 2π), how the different periodic orbits with frequency $2\pi\frac{F_k}{F_{k+1}}$ approach the golden–mean invariant curve.

In order to explore the link between periodic orbits and invariant curves, it is useful to recall some simple notions of number theory and in particular about rational approximants.
For any $\omega \in \mathbf{R}$, let the *continued fraction representation* of ω be defined as the sequence of integer numbers a_j, such that

$$\omega = a_0 + \cfrac{1}{a_1 + \frac{1}{a_2+...}} \;\equiv\; [a_0; a_1, a_2, ...] \;.$$

If $\omega \in \mathbf{R}/\mathbf{Q}$, then the sequence of the $\{a_j\}$'s is infinite; if $\omega \in \mathbf{Q}$, the sequence is finite: $\{a_j\} = \{a_1, ..., a_N\}$. For example, in the case of the golden ratio, one has:

$$\frac{\sqrt{5}-1}{2} \;=\; [0; 1, 1, 1, 1...] \;\equiv\; [0; 1^\infty] \;.$$

Those numbers whose continued fraction expansion is definitely 1, i.e.

$$\alpha = [a_0; a_1, ..., a_N, 1, 1, 1, 1....]$$

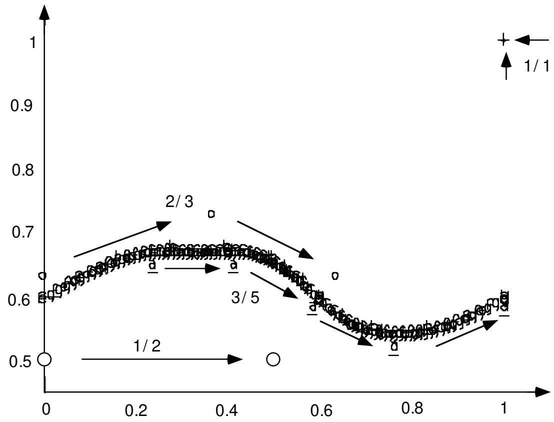

Figure 1: The invariant curve with rotation number $\omega = 2\pi\frac{\sqrt{5}-1}{2}$ and its approximating periodic orbits with frequencies (proportional by a factor 2π) 1, $\frac{1}{2}$, $\frac{2}{3}$, $\frac{3}{5}$ for the mapping (5.29) in the (θ, r)–plane.

for some integer N, are called *noble* numbers. Let $\{\frac{p_j}{q_j}\}$ be the sequence of rational approximants to ω, whose terms are computed as the truncations of the continued fraction expansion, i.e.

$$\begin{aligned}\frac{p_0}{q_0} &= a_0 \\ \frac{p_1}{q_1} &= a_0 + \frac{1}{a_1} \\ \frac{p_2}{q_2} &= a_0 + \frac{1}{a_1 + \frac{1}{a_2}} \\ &\ldots\end{aligned}$$

The rational numbers $\{\frac{p_j}{q_j}\}$ are the *best rational approximants* to the irrational number α.

5.2 Perturbative series expansions

Let us consider the standard map defined in (5.29); by the relations $\theta_{n+1} - \theta_n = r_{n+1}$ and $\theta_n - \theta_{n-1} = r_n$, one obtains that θ must satisfy the equation

$$\theta_{n+1} - 2\theta_n + \theta_{n-1} = \varepsilon \sin\theta_n \ . \tag{5.32}$$

Let us look for a periodic solution with frequency $\omega = 2\pi\,\frac{p}{q}$, satisfying the periodicity conditions

$$\begin{aligned}\theta_{n+q} &= \theta_n + 2\pi p \\ r_{n+q} &= r_n \ .\end{aligned} \tag{5.33}$$

In analogy to (5.31), we parametrize the solution as

$$\theta_n = \varphi_n + u(\varphi_n) \ ,$$

where $\varphi_n \in \mathbf{T}$ and $u(\varphi_n)$ is $2\pi p$–periodic; moreover, the flow is linear with frequency $2\pi\frac{p}{q}$: $\varphi_{n+1} = \varphi_n + 2\pi\frac{p}{q}$ (notice that the conditions (5.33) are trivially satisfied). Next, we expand u in Fourier–Taylor series as

$$u(\varphi_n) \ \equiv \ \sum_{j=1}^{\infty} u_j(\varphi_n)\varepsilon^j \ = \ \sum_{j=1}^{\infty} \varepsilon^j \sum_{l=1}^{\min(j,q)} a_{lj} \sin(l\varphi_n) \ , \tag{5.34}$$

where the real coefficients a_{lj} will be recursively determined by means of (5.32).
Notice that the reason for which the summation ends at $\min(j,q)$ is due to the fact that one needs to avoid zero divisors, as an explicit computation shows.

From (5.32), one finds that u must satisfy the relation

$$u(\varphi_n + 2\pi\frac{p}{q}) - 2u(\varphi_n) + u(\varphi_n - 2\pi\frac{p}{q}) = \varepsilon \sin(\varphi_n + u(\varphi_n)) \ . \tag{5.35}$$

The coefficients a_{lj} can be obtained by inserting the series expansion (5.34) in (5.35) and equating same orders of ε. More precisely, defining $\beta_{l,j}$ such that

$$\sin(\varphi_n + u(\varphi_n)) \equiv \sum_{j=0}^{\infty} \Big(\sum_{l=1}^{j+1} \beta_{l,j+1} \sin(l\varphi_n)\Big) \ \varepsilon^j \ ,$$

one obtains (see [5]) that the coefficients a_{lj} in (5.34) are given by

$$a_{lj} = \frac{\beta_{lj}}{2[\cos(2\pi l\frac{p}{q}) - 1]} \ .$$

At the order ε^q, one meets a singularity whenever $l = q$. In order to bypass this problem, one is forced to select φ_n so that the sine term in (5.34) is zero, i.e.

$$\sin(q\varphi_n) = 0 \ ; \tag{5.36}$$

such choice compensates the zero term (for $l = q$) occurring in

$$\cos(2\pi q \ \frac{p}{q}) - 1 \ .$$

Equation (5.36) provides a value for φ_n as well as for φ_0, since $\varphi_n = \varphi_0 + 2\pi n\frac{p}{q}$. Correspondingly, one has two solutions (modulus 2π), given by

$$\varphi_0 = \frac{\pi}{q} \qquad \text{and} \qquad \varphi_0 = \frac{2\pi}{q} \ .$$

The two solutions are stable or unstable according to the parity of q. In particular $\frac{\pi}{q}$ is stable for q odd, unstable for q even, while the opposite situation occurs for $\frac{2\pi}{q}$. Due to (5.36) the coefficient a_{qq} is not determined by the recursive formulae; however, this term does not contribute to the general solution since $\sin(q\varphi_0) = 0$.

Remark: For an invariant curve with rotation number ω, the conjugating function must satisfy the equation

$$U(\varphi_n + \omega) - 2U(\varphi_n) + U(\varphi_n - \omega) = \varepsilon \sin(\varphi_n + U(\varphi)) \ .$$

Notice that in this case the function $U = U(\varphi_n; \varepsilon)$ depends explicitly on the parametric coordinate φ_n.

6 Numerical investigation of the break–down threshold

6.1 Padé approximants

A numerical investigation of the analyticity domains of periodic orbits is performed using the Padé approximants of order $[N/N]$, i.e. $P_N(\varepsilon)$, $Q_N(\varepsilon)$, such that $\sum_{j=1}^{\infty} u_j \varepsilon^j \equiv \frac{P_N(\varepsilon)}{Q_N(\varepsilon)} + O(\varepsilon^{2N+1})$. The shape of the analyticity domain will be provided by the zero of the denominators. In particular, having fixed a value for φ_0, we consider the series

$$u(\varphi_0) \ = \ \sum_{j=1}^{\infty} u_j(\varphi_0)\varepsilon^j \ , \qquad \varepsilon \in \mathbf{C} \ . \tag{6.37}$$

We compute the Padé approximants of order [200/200], where for consistency the coefficients $u_j(\varphi_0)$ must be calculated with a precision of 400 decimal digits. False poles have been discarded by comparison with the zero's; indeed, we recognize a pole as spurious whenever its coordinates are close to a pole within a suitable tolerance parameter.
We study the periodic orbits generated by the best approximants to the rotation numbers defined as $\gamma = 2\pi[0; 1^\infty]$, $\omega_1 = 2\pi[0; 3, 12, 1^\infty]$, $\omega_2 = 2\pi[0; 2, 10, 1^\infty]$; the corresponding sequences of rational approximants are

$$\begin{gathered}
\{\tfrac{1}{2}, \tfrac{2}{3}, \tfrac{3}{5}, \tfrac{5}{8}, \tfrac{8}{13}, \tfrac{13}{21}, \tfrac{21}{34}, \tfrac{34}{55}, \tfrac{55}{89}, \tfrac{89}{144}, \ldots\} \to \tfrac{\gamma}{2\pi} \\
\{\tfrac{1}{3}, \tfrac{12}{37}, \tfrac{13}{40}, \tfrac{25}{77}, \tfrac{38}{117}, \ldots\} \to \tfrac{\omega_1}{2\pi} \\
\{\tfrac{10}{21}, \tfrac{11}{23}, \tfrac{21}{44}, \tfrac{32}{67}, \tfrac{53}{111}, \tfrac{85}{178}, \ldots\} \to \tfrac{\omega_2}{2\pi} \ .
\end{gathered}$$

Figure 2 (see [5]) shows the Padé approximants of the periodic orbits $\frac{3}{5}, \frac{13}{21}, \frac{34}{55}, \frac{89}{144}$ (times 2π), associated to the mapping (5.29); the inner black region denotes the analyticity domain of the invariant curve with frequency γ. We remark that, as the order q of the periodic orbit grows, the singularities associated to the periodic orbits approach more and more the analyticity domain of the golden–mean invariant curve.

Similarly, the Padé approximants corresponding to ω_1 and ω_2 and to some of their rational approximants are shown, respectively, in Figures 3a and 3b (see [5]).

Let u satisfy (5.35) and let the *radius of convergence* of the series $u(\varphi_0) = \sum_{j=1}^{\infty} u_j(\varphi_0)\varepsilon^j$ be defined as

$$\rho_c(\frac{p}{q}) \ = \ \Big(\limsup_{j\to\infty} \ |u_j(\varphi_0)|^{1/j}\Big)^{-1} \ ,$$

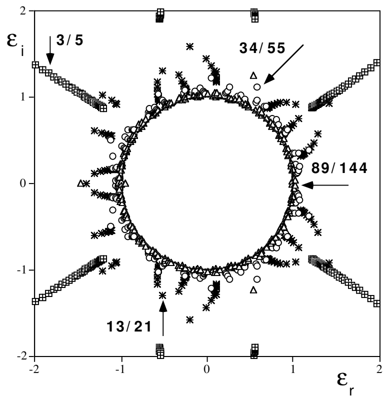

Figure 2: Padé approximants of order [200/200] of the golden mean curve and of the periodic orbits with frequencies $\frac{3}{5}$, $\frac{13}{21}$, $\frac{34}{55}$, $\frac{89}{144}$ (times 2π) for the map (5.29) (after [5]).

while, for ω irrational, we have already defined

$$\rho_c(\omega) \ = \ \inf_{\varphi \in \mathbf{T}} \Big(\limsup_{j \to \infty} \ |U_j(\varphi)|^{1/j} \Big)^{-1} \ .$$

As a byproduct of our numerical analysis, we conjecture that

$$\lim_{k \to \infty} \rho_c(\frac{p_k}{q_k}) \ = \ \rho_c(\omega) \ ,$$

where $\{\frac{p_k}{q_k}\}$ are the rational approximants to ω.

Remark: The evidence that the domains of the approximating periodic orbits tend to a limiting domain seems to suggest that the position of the poles of the invariant curve does not depend on the specific value of the coordinate φ, which must be fixed while computing the Padé approximants.

In order to make our analysis more exhaustive, we investigate also different standard–map like systems; in particular, we consider the following examples:

$$\begin{aligned}
f_{12}: \qquad r_{n+1} &= r_n + \varepsilon(\sin\theta_n + \frac{1}{20}\sin 2\theta_n) \\
\theta_{n+1} &= \theta_n + r_{n+1} \ , \\
f_{13}: \qquad r_{n+1} &= r_n + \varepsilon(\sin\theta_n + \frac{1}{30}\sin 3\theta_n) \\
\theta_{n+1} &= \theta_n + r_{n+1} \ .
\end{aligned}$$

Figure 4 (see [5]) provides the singularities of f_{12} (Figure 4a) and f_{13} (Figure 4b) for $\gamma = 2\pi\frac{\sqrt{5}-1}{2}$.

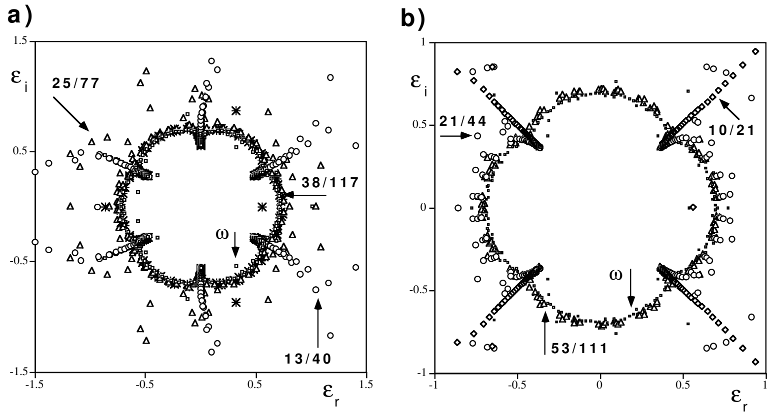

Figure 3: Padé approximants of order [200/200] for the invariant curve with rotation number ω_1 (a) and ω_2 (b) and for some of their rational approximants in the framework of the mapping (5.29) (after [5]).

6.2 Lyapunov's method

In order to estimate the radius of convergence of the Lindstedt series (6.37), we review the algorithm proposed in [5], to which we refer as the *Lyapunov's method.* This technique consists in applying the following procedure:

1) consider discrete values of the small parameter ε from an initial ε_{in} to a final ε_{fin} with a relative increment $(1+h)\varepsilon$;

2) for any of these ε–values, compute the distance d_k between the truncated series at order k calculated at ε with that at $(1+h)\varepsilon$; more precisely, denoting by

$$u^{(k)}(\varphi_0;\varepsilon) \equiv \sum_{j=1}^{k} u_j(\varphi_0)\varepsilon^j \ ,$$

we define the quantity $d_k(\varepsilon)$ as

$$d_k = d_k(\varepsilon) \equiv |u^{(k)}(\varphi_0;(1+h)\varepsilon) - u^{(k)}(\varphi_0;\varepsilon)| \ ;$$

3) for $N \in \mathbf{Z}_+$ large enough, compute the sum

$$s_1 = s_1(\varepsilon) \equiv \frac{1}{N-1}\sum_{k=2}^{N} log\ \frac{d_k}{d_1} \ ;$$

4) plot s_1 versus ε (see Figure 5a). Experimentally one notices that all graphs show an initial almost constant value of s_1 as ε is increased, followed by a small well, and then by a sharp increase with almost linear behaviour;

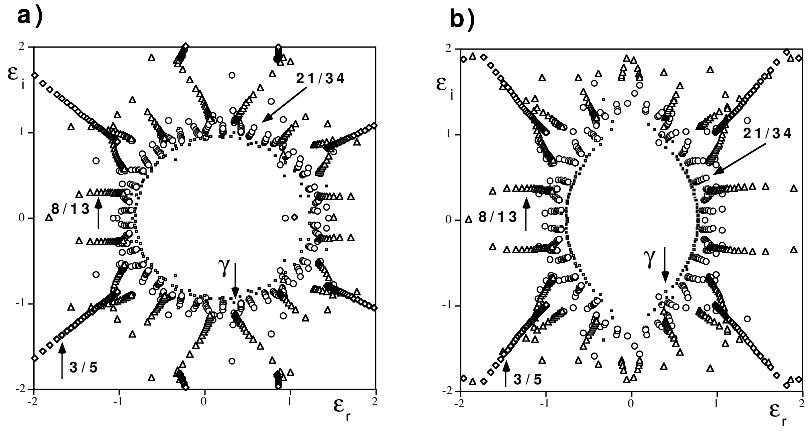

Figure 4: Padé approximants of order [200/200] for the golden mean curve and some rational approximants associated to the mapping f_{12} (a) and f_{13} (b), respectively (after [5]).

5) estimate the analyticity radius as follows (compare with Figure 5b): having fixed the order N (see step 3), at which the series is explicitly computed, and the increment h (see step 1), we interpolate the points before the well with a straigth line. The critical value, say ε_L, is determined as the intersection of such line with the portion of the curve after the minimum is reached.

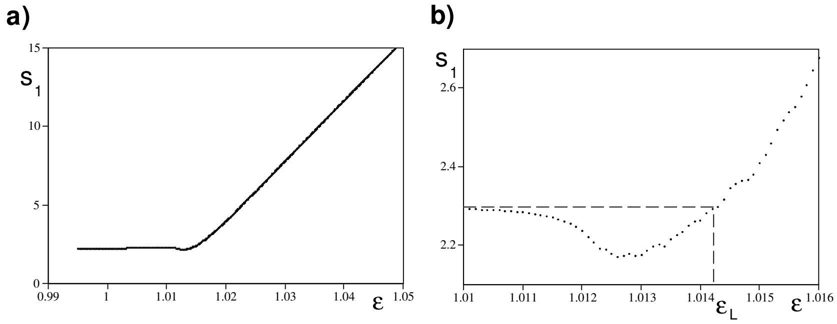

Figure 5: (a) Plot of s_1 versus ε for $\omega = 2\pi\frac{34}{55}$, $N = 800$, $h = 0.001$; (b) zoom of (a) for $1.01 \leq \varepsilon \leq 1.016$ and computation of ε_L (after [5]).

Figure 5 (see [5]) shows an implementation of such algorithm for the standard mapping (5.29) and the frequency $\omega = 2\pi\frac{34}{55}$; the parameters has been set as $N = 800$ and $h = 0.001$.

6.3 Greene's method

Let $\mathcal{C}_{\varepsilon,\omega}$ denote the invariant curve with irrational frequency ω. We define the critical threshold at which $\mathcal{C}_{\varepsilon,\omega}$ breaks down as

$$\begin{aligned}\varepsilon_c(\omega) = \quad & \sup\{\varepsilon' \geq 0 : \text{for any } \varepsilon'' < \varepsilon',\ \text{there exists an analytic} \\ & \qquad\qquad \text{invariant curve } \mathcal{C}_{\varepsilon'',\omega}\}\ .\end{aligned}$$

The most widely accepted numerical technique to compute $\varepsilon_c(\omega)$ is Greene's method ([8]), which is based on the analysis of the stability of the periodic orbits approaching $\mathcal{C}_{\varepsilon,\omega}$. In order to investigate the stability character of a periodic orbit with frequency $2\pi\frac{p}{q}$ (for some p, $q \in \mathbf{Z}$), we look at the eigenvalues of the monodromy matrix

$$M \ = \ \prod_{i=1}^{q} \begin{pmatrix} 1+\varepsilon\cos(\theta_i) & 1 \\ \varepsilon\cos(\theta_i) & 1 \end{pmatrix}\ ,$$

where $(\theta_1, ..., \theta_q)$ are successive points on the periodic orbit associated to the mapping (5.29). From the area–preserving property, one has that $\det M = 1$. Let T be the trace of M, whose eigenvalues are solutions of the equation: $\lambda^2 - T\lambda + 1 = 0$. Then, if $|T| < 2$, the eigenvalues of M are complex conjugates on the unit circle and the periodic orbit is stable. On the contrary, if $|T| > 2$ the eigenvalues are real and the periodic orbit is unstable.

To be concrete, let us fix a periodic orbit with frequency $2\pi\frac{p}{q}$, such that it is elliptic for small values of ε (as well as for $\varepsilon = 0$). As ε increases, the trace of the matrix M exceeds eventually 2 in modulus and the periodic orbit becomes unstable.
Figure 6a (see [5]) shows the quantity $\rho_{Gr}(\frac{p_k}{q_k})$, which corresponds to the value of ε marking the transition from stability to instability of the periodic orbit with frequency $2\pi\frac{p_k}{q_k}$. We selected the sequence of rational approximants to the golden ratio γ and we represented with a dotted line the estimated break–down value of $\mathcal{C}_{\varepsilon,\gamma}$. Figure 6$b$ provides a comparison between Greene's and Lyapunov's methods, by showing the plot of the relative error of the quantities $\rho_c(\frac{p_k}{q_k})$ and $\rho_{Gr}(\frac{p_k}{q_k})$.

6.4 Results

In the framework of the standard map (5.29), we show some results on the behaviour of the invariant curves with frequencies γ, ω_1, ω_2, where $\gamma = 2\pi[0;1^\infty]$, $\omega_1 = 2\pi[0;3,12,1^\infty]$, $\omega_2 = 2\pi[0;2,10,1^\infty]$. We have implemented the three techniques presented in the previous sections, i.e. Padé, Greene and Lyapunov. Such methods depend on the choice of some parameters and of tolerance errors. In particular, Lyapunov's method depends on the order N of the truncation and on the increment h of the perturbing parameter ε. For a fixed N the agreement of the three methods is almost optimal taking a suitable value of the increment, typically $h = 0.001$. Table 1 shows a comparison of the three methods for the golden ratio approximants of the standard map (5.29). The series have been computed up to $N = 800$ and the increment of Lyapunov's method has been set to $h = 10^{-3}$ (compare with [5]).

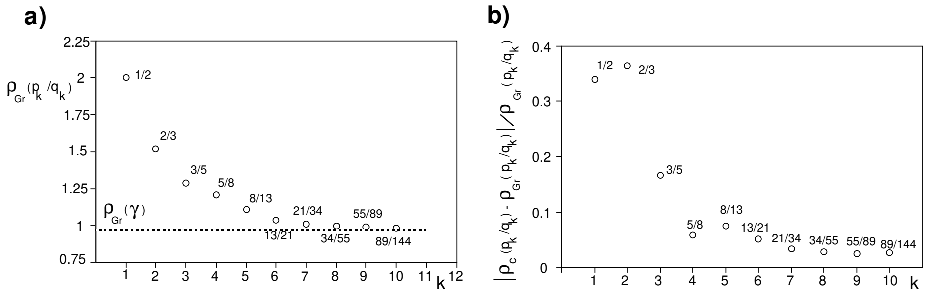

Figure 6: (a) $\rho_{Gr}(\frac{p_k}{q_k})$ versus the order k pertaining the rational approximants to the golden ratio; the dotted line represents Greene's threshold about equal to 0.971635. (b) The relative error associated to $\rho_c(\frac{p_k}{q_k})$ and $\rho_{Gr}(\frac{p_k}{q_k})$ for some rational approximants to the golden ratio (after [5]).

p/q	Greene	Padé	Lyap.:$h = 10^{-3}$
2/3	1.5176	2.0501	2.0584
3/5	1.2856	1.4873	1.4913
5/8	1.1485	1.2495	1.2561
8/13	1.0790	1.1440	1.1492
13/21	1.0353	1.0753	1.0766
21/34	1.0106	1.0366	1.0397
34/55	0.9953	1.0115	1.0142
55/89	0.9862	0.9974	0.9960
89/144	0.9832	0.9909	0.9897

Table 1: Comparison of Greene's, Padé's and Lyapunov's methods for the rational approximants to the golden ratio in the framework of the mapping (5.29) (after [5]).

Table 2 (see [5]) provides the results for the invariant curve associated to the standard map (5.29) with frequency equal to ω_1; we underline the good agreement between Padé's and Lyapunov's methods, providing estimates of the analyticity radius. Due to the length of the calculations, it was possible to compute only the first few approximants while applying Padé's method (up to 38/117 in Table 2 and up to 85/178 in Table 3).

p/q	Greene	Padé	Lyap.:$h = 10^{-3}$
12/37	0.7486	0.5730	0.57513
13/40	0.7322	0.5447	0.54658
25/77	0.7232	0.5579	0.56063
38/117	0.7145	0.5539	0.55580
63/194	0.7134		0.55755
101/311	0.7085		0.55688
164/505	0.7073		0.55715
265/816	0.7066		0.55706
429/1321	0.7056		0.55705

Table 2: Same as Table 1 for the invariant curve with frequency ω_1 (after [5]).

Similarly, we report in Table 3 the results for the invariant curve associated to the standard map (5.29) with frequency equal to ω_2 (compare with [5]).

p/q	Greene	Padé	Lyap.:$h = 10^{-3}$
10/21	0.7487	0.5395	0.54165
11/23	0.7198	0.5008	0.49557
21/44	0.7060	0.5158	0.51795
32/67	0.6919	0.5084	0.51058
53/111	0.6869	0.5116	0.51354
85/178	0.6842	0.5105	0.51239
138/289	0.6801		0.51281
223/467	0.6785		0.51265
361/756	0.6781		0.51271
584/1223	0.6771		0.51268

Table 3: Same as Table 1 for the invariant curve with frequency ω_2 (after [5]).

In the cases of the mappings f_{12} and f_{13}, we found the results reported in Figure 7 (see [5]), where the abscissa k refers to the order of the approximant p_k/q_k of the golden ratio: for example, $k = 1$ corresponds to 2/3, while $k = 9$ corresponds to 89/144. With reference to Figure 7, the break–down threshold, as computed by Greene's method (squares), amounts to $\varepsilon_c(\gamma) = 1.2166$ for f_{12} (see Figure 7a) and to $\varepsilon(\gamma) = 0.7545$ for f_{13} (see Figure 7b). The Lyapunov's method has been applied with a series truncated at $N = 800$ and for $h = 0.01$ (crosses) and $h = 0.001$ (triangles). Padé approximants of order [200/200] have been also computed (diamonds). Due to the length of the calculations, it was possible to compute only the first few approximants (up to 21/34) by applying Padé's method.

The results indicate that there is a good agreement between all methods as far as the approximants to the golden mean curve associated to (5.29) are analyzed. In such case the analyticity

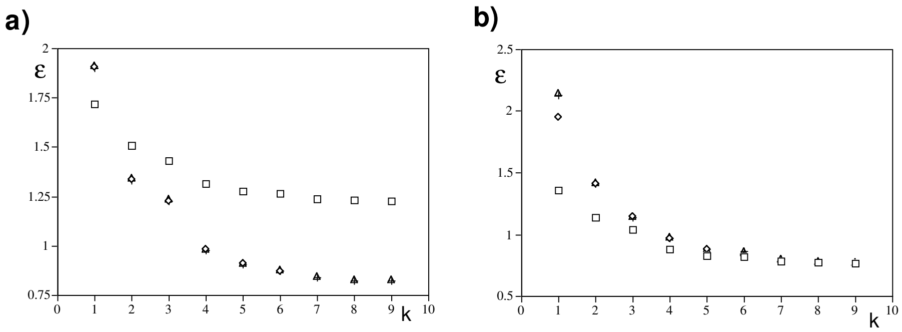

Figure 7: Comparison of the results for the mappings f_{12} (a) and f_{13} (b) and for some rational approximants labelled by the index k; square: Greene's value, diamond: Padé's results, cross: Lyapunov's indicator s_2 (after [5]).

domain is close to a circle, so that the intersection with the positive real axis (providing an estimate of Greene's threshold) almost coincides with the analyticity radius, which is obtained implementing Padé's and Lyapunov's methods.
Such situation does not hold whenever the analyticity domain is not close to a circular shape. This happens, for example, when the invariant curves with rotation numbers $\omega_1 = 2\pi\ [0; 3, 12, 1^\infty]$ and $\omega_2 = 2\pi\ [0; 2, 10, 1^\infty]$ are considered; in these cases the two thresholds (break–down value and analyticity radius) are markedly different.

References

[1] Arnold V.I.: *Proof of a Theorem by A.N. Kolmogorov on the invariance of quasi–periodic motions under small perturbations of the Hamiltonian*, Russ. Math. Surveys **18**, 9 (1963)

[2] Arnold V.I. (editor): *Encyclopedia of Mathematical Sciences*, Dynamical Systems III, Springer–Verlag **3** (1988)

[3] Baker G. A. Jr., Graves-Morris P.: *Padé Approximants*, Cambridge University Press, New York (1996)

[4] Celletti A., Chierchia L.: *KAM Stability and Celestial Mechanics*, Preprint (2003), *http://www.mat.uniroma3.it/users/chierchia/PREPRINTS/SJV_03.pdf*

[5] Celletti A., Falcolini C.: *Singularities of periodic orbits near invariant curves*, Physica D **170**, n. 2, 87 (2002)

[6] Chirikov B.V., *A universal instability of many dimensional oscillator systems*, Physics Reports **52**, 264–379 (1979)

[7] Falcolini C., de la Llave R.: *A rigorous partial justification of the Greene's criterion*, J. Stat. Phys., **67**, 609 (1992)

[8] Greene J.M.: *A method for determining a stochastic transition*, J. Math. Phys. **20** (1979)

[9] Hénon M.: *Explorationes numérique du problème restreint IV: Masses egales, orbites non periodique*, Bullettin Astronomique **3**, 1, fasc. 2, 49–66 (1966)

[10] Kolmogorov A.N.: *On the conservation of conditionally periodic motions under small perturbation of the Hamiltonian*, Dokl. Akad. Nauk. SSR **98**, 469 (1954)

[11] MacKay R. S.: *Greene's residue criterion*, Nonlinearity, **5**, 161–187 (1992)

[12] Moser J.: *On invariant curves of area-preserving mappings of an annulus*, Nach. Akad. Wiss. Göttingen, Math. Phys. Kl. II **1**, 1 (1962)

[13] Poincaré H.: *Les Methodes Nouvelles de la Mechanique Celeste*, Gauthier Villars, Paris (1892)

[14] Szebehely V.: *Theory of orbits*, Academic Press, New York and London (1967)